South American Journal of HERPETOLOGY

VOLUME 13 | ISSUE 2 | AUGUST 2018

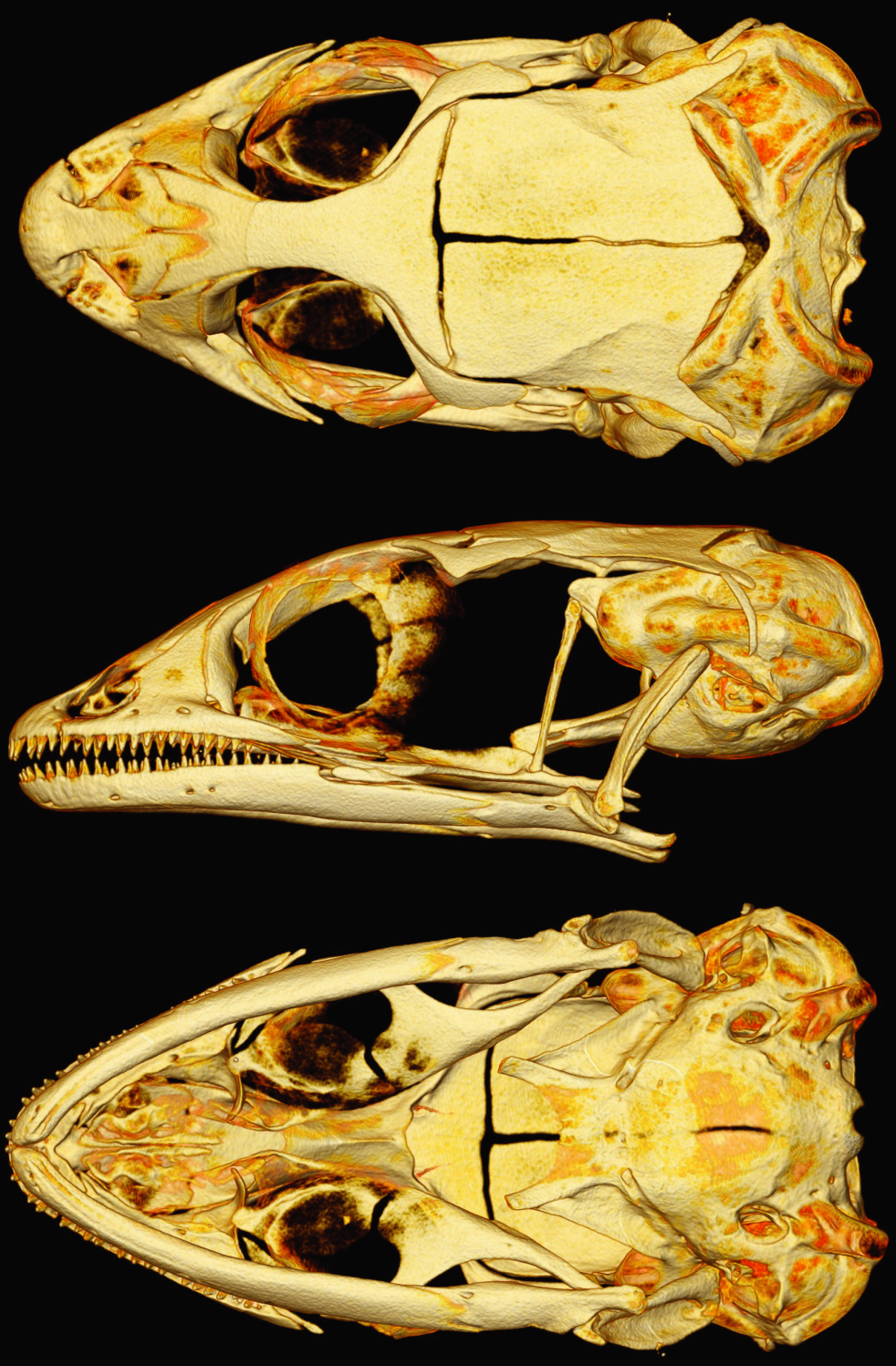

SBH
SOCIEDADE BRASILEIRA DE HERPETOLOGIA

The Tiny Skull of the Peruvian Gecko *Pseudogonatodes barbouri* (Gekkota: Sphaerodactylidae) Obtained via a Divide-And-Conquer Approach to Morphological Data Acquisition

Author(s): Aaron M. Bauer, Mallika Beach-Mehrotra, Yarima Bermudez, Geneva E. Clark, Juan D. Daza, Elizabeth Glynne, David Hagyari, Jennifer M. Harnden, Nicholas Holovacs, Andre Kanasiro, Amanda J. Lofthus, Zachary W. Pierce, Ryan Aaliyah, Samreena Syed, Maria C. Vallejo-Pareja, Bethany A. Walker and James Willett

Source: South American Journal of Herpetology, 13(1):102-116.
Published By: Brazilian Society of Herpetology
URL: http://www.bioone.org/doi/full/10.2994/SAJH-D-17-00113.1

South American Journal of Herpetology, 13(2), 2018, 102–116

The Tiny Skull of the Peruvian Gecko *Pseudogonatodes barbouri* (Gekkota: Sphaerodactylidae) Obtained via a Divide-And-Conquer Approach to Morphological Data Acquisition

Aaron M. Bauer[1], Mallika Beach-Mehrotra[2], Yarima Bermudez[2], Geneva E. Clark[2], Juan D. Daza[2,*], Elizabeth Glynne[2], David Hagyari[2], Jennifer M. Harnden[2], Nicholas Holovacs[2], Andre Kanasiro[2], Amanda J. Lofthus[2], Zachary W. Pierce[2], Ryan Aaliyah[2], Samreena Syed[2], Maria C. Vallejo-Pareja[2], Bethany A. Walker[2], James Willett[2]

[1] *Biology Department, Villanova University, 800 Lancaster Avenue, Villanova, Pennsylvania 19085, USA.*
[2] *Department of Biological Sciences, Sam Houston State University, 1900 Avenue I Lee Drain Building, Suite 300, Huntsville, Texas 77341, USA.*
[*] *Corresponding author. Email: juand.daza@gmail.com*

Abstract. The Peruvian sphaerodactyl gecko, *Pseudogonatodes barbouri,* is among the smallest reptile species in South America. Morphological information about this species, or even the genus, is limited. In this study, we produced a bone-by-bone description from the skull and atlantoaxial complex to contribute new phenotypic information about this poorly known lizard. To achieve this objective, we employed a divide-and-conquer approach in which each author digitally isolated one or two bones from the skull and produced a written description of these elements, thereby reducing 3D imaging processing and description to a fraction of time. In addition to a reduced phalanx in the fourth toe of both the hand and foot, the genus is characterized by having nasal bones with a broad lateral wing, an ectopterygoid that clasps the pterygoid, and an anterior shifting of the paroccipital process and as consequence the position of the quadrate, and squamosal not participating in the quadrate suspension. There are also modifications in fenestration and foramina and a trend towards synostosis of the jaw bones (e.g., coronoid + splenial, compound bone + surangular). *Pseudogonatodes* bears four long processes on the intercentrum of the axis; which is a character of New World sphaerodactyls.

Keywords. CT scan; High-resolution computer tomography; Lizard; Osteology; Squamata.

INTRODUCTION

Pseudogonatodes Ruthven, 1915 is one of six genera of sphaerodactyl geckos, a clade of mostly miniaturized New World lizards nested within Sphaerodactylidae Underwood, 1954 distributed in the northwestern part of South America (Gamble et al., 2008, 2011), including portions of Colombia, Venezuela, Guyana, Suriname, French Guyana, Ecuador, Peru, and Brazil (Kluge, 1995; Avila-Pires and Hoogmoed, 2000). The genus comprises seven species (Uetz et al., 2017), all of which have limited distributions except the widespread *P. guianensis* Parker, 1935.

Morphological data for the genus are very limited, as only a few studies have discussed its osteology (Noble, 1921a; Kluge, 1995; Daza et al., 2008; Daza and Bauer, 2012) or scalation (Ruthven, 1916; Noble, 1921a; Parker, 1926; Vanzolini, 1957; Avila-Pires, 1995; Kluge, 1995). Toe morphology was originally used to distinguish the genus, which is characterized by short, slender digits that are slightly depressed at the base (Ruthven, 1915), a trait that is consistent with the loss of a phalangeal element in the fourth digit of the hands (Gasc, 1976; Kluge, 1995) and feet (Gamble et al., 2011).

In this paper, we study in detail the skull morphology of *Pseudogonatodes barbouri* Noble, 1921a in an effort to contribute to the knowledge of this obscure genus of sphaerodactyl geckos. Detailed descriptions of the skull of sphaerodactyl geckos are available for the genera *Sphaerodactylus* Wagler, 1830 (Daza et al., 2008) and *Chatogekko* Gamble et al., 2011. The main goals of this paper are to describe and illustrate each bone from the skull of this species and to discuss some of the unique features in the context of the New World sphaerodactyls. To achieve these goals, we used high-resolution computer tomography images and provide articulated and bone-by-bone descriptions. This method facilitates studying miniaturized species, which are more difficult (or nearly impossible) to examine using other methods (e.g., skeletonization or clearing and staining, see Daza et al., 2008).

How to cite this article: Bauer A.M., Beach-Mehrotra M., Bermudez Y., Clark G.E., Daza J.D., Glynne E., ... Willett J. 2018. The tiny skull of the Peruvian gecko *Pseudogonatodes barbouri* (Gekkota: Sphaerodactylidae) obtained via a divide-and-conquer approach to morphological data acquisition. *South American Journal of Herpetology* 13:102–116. doi:10.2994/SAJH-D-17-00113.1

Submitted: 18 December 2017
Accepted: 10 February 2018
Available Online: 21 May 2018

Handling Editor: Taran Grant
http://doi.org/10.2994/SAJH-D-17-00113.1

MATERIALS AND METHODS

An ethanol preserved paratype of *Pseudogonatodes barbouri* (MCZ R-14385) was studied in detail. The specimen was collected in 1916 from Bella Vista, northwestern Peru, as part of the Harvard Peruvian Expedition by Gladwyn Kingsley Noble. High-resolution computer tomography (HRCT) scans were obtained at The University of Texas High-Resolution CT Facility (UTCT) using a 4X objective (99 kV, 10W) from an Xradia system. The stack of images was loaded into Avizo Lite 9.4 (Thermo Fisher Scientific™, 2017), where 3D models were generated for the articulated skull and for each individual bone. All segmentation files (*.am) were compiled in a master copy to ensure the same volume parameters were controlled for quality and uniformity of the volumes.

This project is the outcome of a mixed graduate and undergraduate course (Visual Methods for Studying Morphology and Evolution), and all the students in this class are co-authors of the paper, including 11 Master of Sciences students and four upper-level undergraduates. Only four of the students had prior familiarity with squamate morphology. The course was taught in the Fall semester of 2017 (September to December) at Sam Houston State University in Huntsville, Texas, and this project was one of four modules that included learning other computer packages.

A divide-and-conquer strategy was performed to expedite segmentations, and one or two skull bones were assigned to each author to allow work to be done simultaneously. This approach allowed almost all 3D models to be obtained in about a 1 week (8–15 November 2017). This approach was also used to describe each of the individual bones, and all authors provided feedback on the final version of the manuscript. Annotations were made in Adobe Illustrator CC 22.0.1 (Adobe Systems Incorporated, 2017) following the anatomical terminology of Daza et al. (2008), Evans (2008), Gamble et al. (2011), and Olori and Bell (2012). In addition to the models produced here, a model of the articulated skull was entered into MorphoSource (Duke University, 2017: Identifier: S9529), where the specimen can be seen from any angle. Cross sections and the original dataset are also available in the MorphoSource website (https://www.morphosource.org).

RESULTS

Overall description of the skull

The skull (Figs. 1A–C, 2A–F) is longer than wide, with a 1:1 proportion between the muzzle unit and the parietal + neurocranium unit, as is typical of miniaturized sphaerodactyls (Daza et al., 2008). The cranium is wedge shaped and has open lateral borders, with the space for the orbit and the supratemporal and infratemporal fossae combined. The anterior tip of the cranium is formed only by the premaxilla, and the osseous nares are wide and ovoid. The lacrimal foramen opens laterally. The quadrate is located just posteroventral to the anterior ampullae. The quadrate is streptostylic and is suspended from a reduced paroccipital process, but without participation of the squamosal. The quadrate is also slightly convex, defining a conch that is far anterior to the middle ear, indicating that the volume of the middle ear region is ample in the species. The fenestra ovalis is larger than the footplate of the otostapes.

The cranium has a well-developed mesokinetic plane as indicated by a nearly horizontal frontoparietal suture. The parietal covers the braincase, with some gaps at the frontoparietal and interparietal sutures. There is also a small gap posteromedially, leaving the medial border of the supraoccipital exposed. The parietal does not contact the prootic via the descending parietal process or the supraoccipital. The infraorbital fenestrae have the characteristic "D" shape of sphaerodactyls (Daza et al., 2008). The palate has well-developed incisive fenestra between the premaxillary shelf and the vomer (Gamble et al., 2011), and a continuous fenestra exochoanalis that is continued into a hemitubular palatine (duplicipalatine condition). The interpterygoid vacuity extends slightly into the intervomerine suture and is constrained anteriorly and wide posteriorly, remaining bounded by the diverging and nearly straight medial margin of the pterygoids. There is a limited space between the posteromedial margin of the pterygoid and the crista prootica. The braincase is proportionally large, with protruding horizontal semicircular canals forming the posterior margin. The braincase shows a narrow, ventral area that corresponds to the position of the embryonic basicranial fenestra that is visible depending on the volume rendering threshold.

The cranium appears narrow in anterior view with the snout tapered and slender. The anterolateral orientation of the sclerotic rings indicates that the eyes have overlapping visual fields. In posterior view the cranium is significantly wider than in anterior view, and the foramen magnum is large and forms a rounded-edged pentagon.

The jaw (Fig. 2C–F) is elongate, mediolaterally compressed, and mainly straight, with only a slight curvature near the symphyseal region. The coronoid eminence is low, not exceeding the height of the dentary teeth. Postdentary elements have undergone synostosis; the coronoid morphology suggests two alternatives: (1) the splenial is fused to coronoid, or (2) the splenial is lost and the coronoid develops an anteromedial foot, which forms the wall of the Meckelian canal. The remaining portion of the jaw is formed by a fused compound bone (articular, prearticular, and angular; Daza et al., 2008) and surangular.

In the CT scans the hyoid apparatus was not completely visible, perhaps due to its cartilaginous nature. Published illustrations of other sphaerodactyl species are

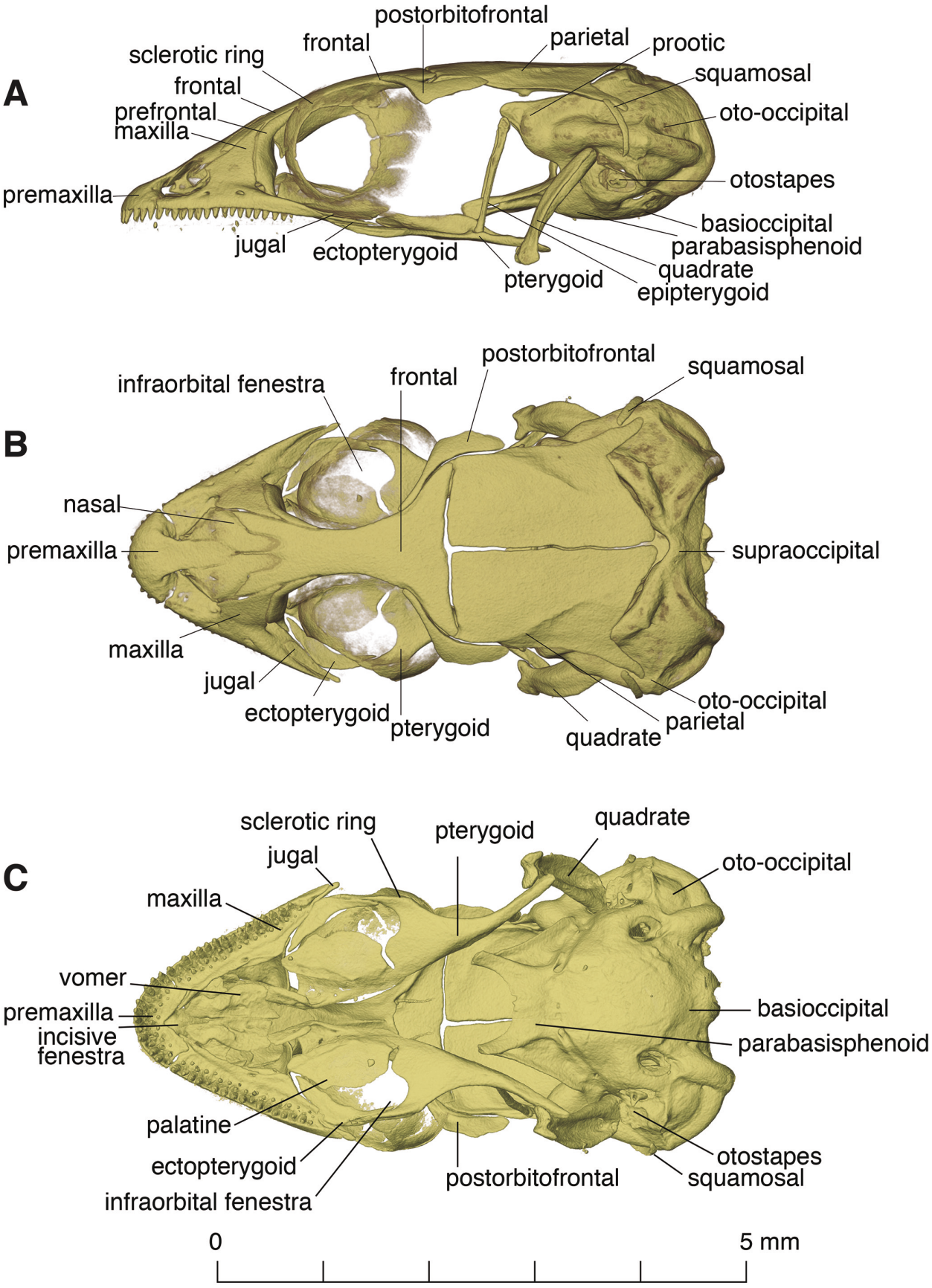

Figure 1. *Pseudogonatodes barbouri* (MCZ R-14385). Skull in **(A)** lateral, **(B)** dorsal, and **(C)** ventral view.

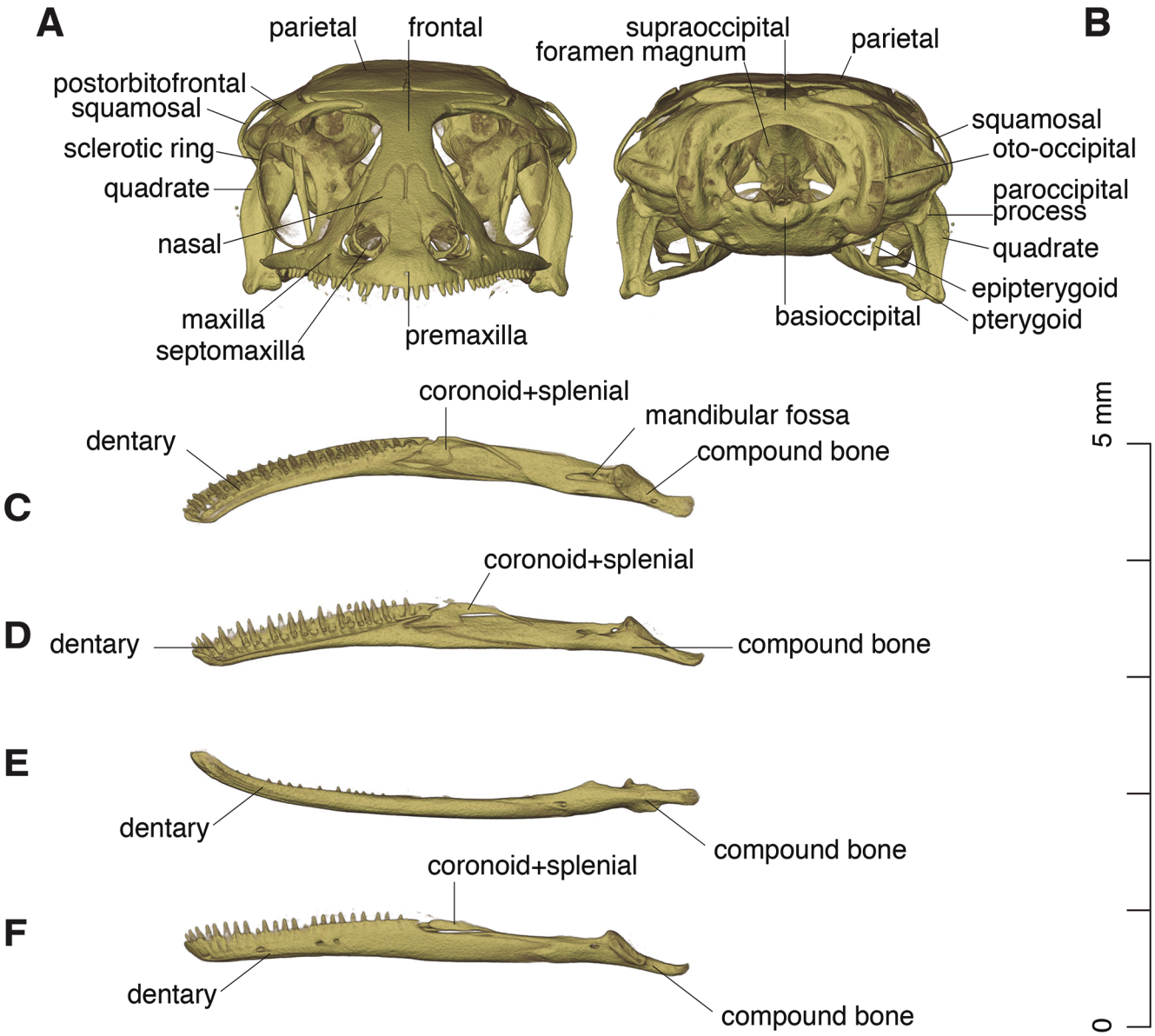

Figure 2. *Pseudogonatodes barbouri* (MCZ R-14385). Skull in **(A)** anterior, and **(B)** posterior view, jaw in **(C)** dorsal, **(D)** medial, **(E)** ventral, and **(F)** lateral view.

available (Noble, 1921b; Gamble et al., 2011): *Sphaerodactylus macrolepis* Günther, 1859 and *Chatogekko amazonicus* (Andersson, 1918), showing differences in the length of the second ceratobranchial, nearly subequal to the glossohyal in *S. macrolepis* Günther, 1859 and about half the length of the glossohyal in *C. amazonicus* (Andersson, 1918). Another difference between these two species is the apparent connection of the second epibranchial with the second ceratobranchial in *Sphaerodactylus* and the completely independent structure in *C. amazonicus* (Andersson, 1918) (Gamble et al., 2011). A revision of the hyoid apparatus in sphaerodactyls is needed, since the mentioned condition in *S. macrolepis* is rare, as pointed out by Noble (1921b). Unfortunately, we could not add more information to this subject based on the CT scanned specimen.

Description of isolated bones

Premaxilla (Fig. 3A–E)

An unpaired bone that lies anterior to the snout, contacting nasals, maxillae, and vomer. The ventral portion of the bone bears thirteen tooth loci. The specimen shows 2–3 replacement rows of tooth buds. The ascending nasal process contacts ventrally the anterior portion of the nasals. The overlap of the premaxilla with the nasals is a butt-lap joint which provides a rigid connection that might allow for a sturdier snout (Daza et al., 2008). The septonasal crest is well defined and fits between the anterior portion of the nasal bones. The palatal process extends medially to contact the vomer. The maxillary facet

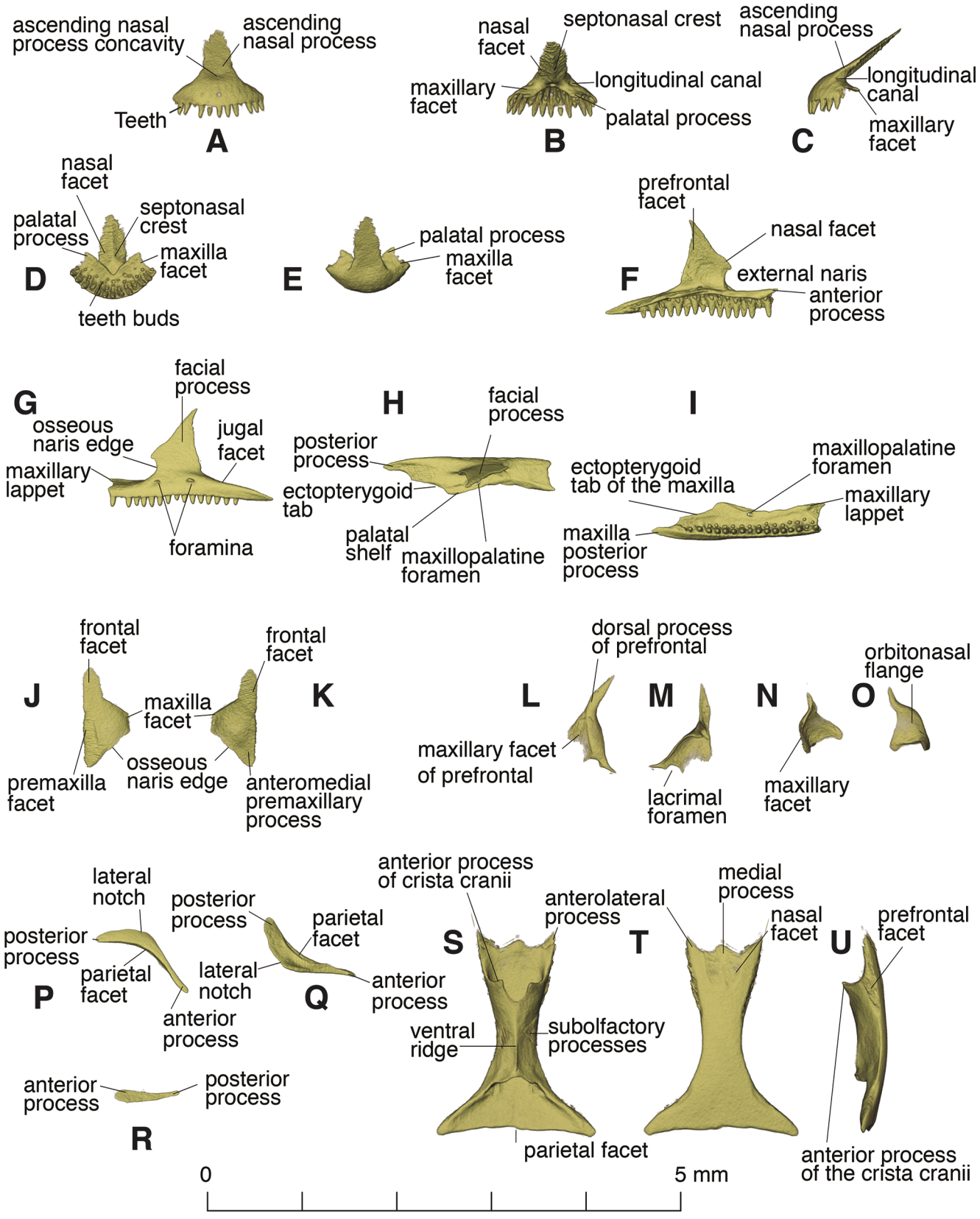

Figure 3. *Pseudogonatodes barbouri* (MCZ R-14385). Premaxilla in **(A)** anterior, **(B)** posterior, **(C)** lateral, **(D)** ventral, and **(E)** dorsal view. Left maxilla in **(F)** medial, **(G)** lateral, **(H)** dorsal, and **(I)** ventral view. Left nasal in **(J)** dorsal and **(K)** ventral view. Left prefrontal in **(L)** lateral, **(M)** medial, **(N)** anterior, and **(O)** posterior view. Left postorbitofrontal in **(P)** dorsal and **(Q)** ventral view. **(R)** Left jugal in dorsal view. Frontal in **(S)** ventral, **(T)** dorsal, and **(U)** lateral view.

forms the posterior-most portion of the palatal process. The maxilla facet is posterior to the more lateral teeth. On the ventral side of the premaxilla there is a notch in between the palatal processes that exposes the septonasal crest.

Maxilla (Fig. 3F–I)

This bone contacts the premaxilla anteriorly, nasal anterodorsally, frontal dorsomedially, prefrontal posterodorsally, jugal posteromedially, and ectopterygoid medially. The left and right maxillae each bear 16 tooth loci. Both the resorption pits of the teeth and the tooth buds are close to the medial shelf ventral surface. The medial shelf approaches the vomer to form the lateral border of the fenestra exochoanalis. It also forms the floor of the osseous naris anterodorsally and the anterolateral edge of the choana. The anteromedial maxillary lappet is an acute triangle with a 35° internal angle and overlaps the maxillary process of the premaxilla; its medial edge is slightly overlapped by the septomaxilla. The maxillopalatine foramen opens dorsally at the junction of the palatal shelf and the medial portion of facial process; it opens ventrally near the medial edge of the palatal shelf. The facial process is tall and roughly triangular in shape, with a steep posterior border of the osseous naris; the posterior edge forms the anterior border of the lacrimal foramen. The posterior margin of the facial process is tall and nearly vertical, deflecting slightly towards its highest point. The facial process overlaps briefly the nasal anterodorsally, and the prefrontal lateromedially. The posterior process tapers posteriorly and is overlapped by the jugal.

Nasal (Fig. 3J–K)

This bone contacts the premaxilla anterodorsally, the maxilla laterodorsally, and the frontal posterolaterally. It has a distinctive lateral laminar wing that contacts the maxilla. The bone is slightly convex. Its anterolateral margin is oblique and expands into the lateral wing. On the dorsal surface there is a shallow shelf to support the premaxilla.

Prefrontal (Fig. 3L–O)

The prefrontal is a crescent shaped bone that contacts the maxilla at two points, anterolaterally at the facial process and ventrally, perpendicular to the posterior process; contact with the maxilla is interrupted by the lacrimal foramen. The prefrontal also contacts the frontal posteromedially. The prefrontal has a medial orbitonasal flange that separates the nasal cavity from the eye socket. At its contact with the maxilla, it forms the dorsal and medial border of the triangular shaped lacrimal foramen. The bone has two acute processes, one that flanks the frontal and one that abuts the maxilla perpendicularly. The maxillary facet seems to have ridged margins, but this is due to the thickness of the bone, which is very thin, and might be an artifact data visualization program. The dorsal process of the prefrontal is spike-like and lies lateral to the anterior portion of the frontal bone.

Postorbitofrontal (Fig. 3P–Q)

We follow the interpretation of this bone as the fusion of postorbital and postfrontal (see Daza et al., 2008 for a discussion of this topic). The postorbitofrontal is a boomerang-shaped bone that contacts the frontal and parietal medially. The anterior process is long and narrow, and the posterior process is nearly twice as wide. The bone clasps the frontoparietal suture, extending the roofing of the braincase laterally.

Jugal (Fig. 3R)

The jugal is a long thin bone that is nestled dorsomedially to the posterior process of the maxilla. The anterior process of the jugal is wide and rounded. The posterior process of the jugal tapers into a narrow rounded point that extends slightly beyond the maxilla. The jugal is slightly curved as it follows the curvature of the maxilla. The jugal forms a diarthrosis with the adjacent ectopterygoid bone.

Frontal (Figs. 3S–U)

The frontal bone is unpaired and tubular with a nearly hourglass shape. This bone contacts the nasals anterodorsally, prefrontals laterally, postorbitofrontal posterolaterally, and the parietals posteriorly. The facets that connect with the dorsal process of the prefrontal are well defined on the bone surface. Anterodosally the facets for the nasals are well defined too. The anterior portion of this bone has two anterolateral processes and a mound-shaped medial process. In lateral view, the anterior end has a deep concavity that is occupied by the olfactory lobes; this concavity is formed by the anterior extension of the anterolateral process of the frontal and the short flange of the anterior process of the crista cranii. There are two concave depressions on either side of the posterior end of the bone corresponding to the orbital rim. The posterior end is slightly bowed, forming a nearly straight and movable frontoparietal suture.

Parietal (Figs. 4A–D)

The parietal is paired and roughly rectangular. It roofs the braincase and contacts the frontal anteriorly, postorbitofrontal anterolaterally, and has a ligamentous connection with the squamosal posterolaterally. The

frontal facet develops a short anterolateral process that hinges this bone to the frontal to form the movable (mesokinetic) frontoparietal joint. The bone develops a subtle posteromedial crease that continues onto the posterolateral process. The posterolateral process is blade-like and is supported by the otooccipital portion of the braincase.

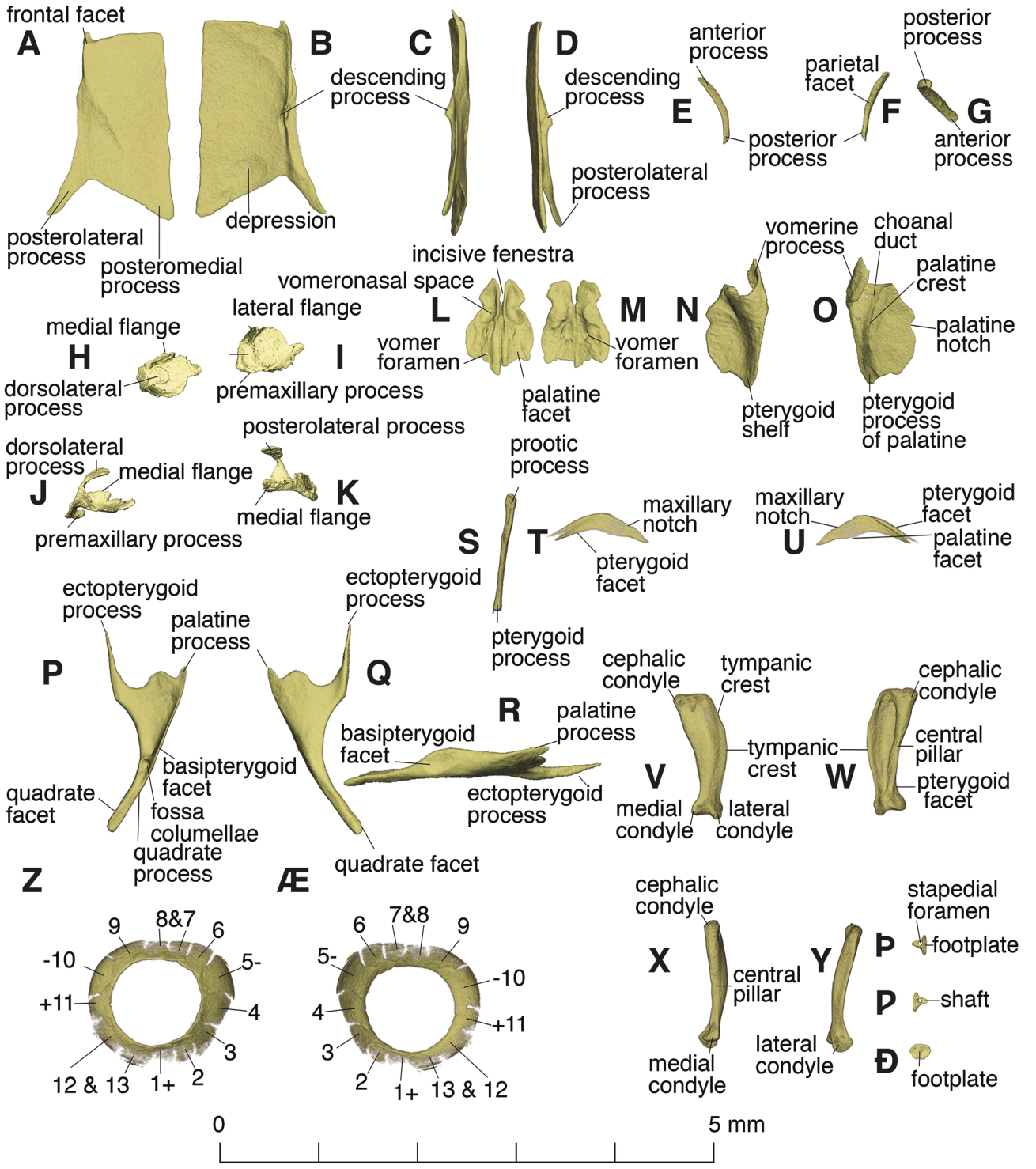

Figure 4. *Pseudogonatodes barbouri* (MCZ R-14385). Left parietal in **(A)** dorsal, **(B)** ventral, **(C)** lateral, and **(D)** medial view. Left squamosal in **(E)** lateral, **(F)** dorsal, and **(G)** medial view. Left septomaxilla in **(H)** dorsal, **(I)** ventral, **(J)** lateral, and **(K)** medial view. Vomer in **(L)** dorsal, and **(M)** ventral view. Left palatine in **(N)** dorsal, and **(O)** ventral view. Left pterygoid in **(P)** ventral, **(Q)** dorsal, and **(R)** medial view. **(S)** Left epipterygoid. Left ectopterygoid in **(T)** dorsal and **(U)** ventral view. Left quadrate in **(V)** anterior, **(W)** posterior, **(X)** medial, and **(Y)** lateral view. Sclerotic ring in **(Z)** lateral and **(Æ)** medial view. Left otostapes in **(Þ)** dorsal, **(ÞÞ)** ventral, and **(ÐÐ)** medial view.

On the ventrolateral side, the parietal has a longitudinal ridge that gives rise to the descending process. The descending process is directed toward the crista alaris, but without contacting it.

Squamosal (Figs. 4E–G)

A slender, nearly vertically oriented, j-shaped bone bridging the posterolateral process of the parietal and the horizontal semicircular canal bulge of the braincase. This bone forms the dorsolateral border of a reduced postemporal fenestra. Distinctively, the squamosal makes no contact with the quadrate bone but its posterior process ends curving along and under the horizontal semicircular canal of the braincase, just above the fenestra ovalis.

Septomaxilla (Figs. 4H–K)

The septomaxilla is a very thin paired bone that occupies the nasal cavity and that contacts the vomer ventrally and the maxilla laterally. The bone has one dorsolateral process and its main body is convex. The dorsolateral process contacts the medial side of the facial process of the maxilla. The space ventral to the septomaxilla accommodates the mushroom body. The remaining space between the septomaxillae is occupied by the nasal septum cartilage.

Vomer (Figs. 4L–M)

The vomer seems at least partially fused. The bone is roughly flat and its overall contour resembles a butterfly. This bone contacts the premaxilla anteriorly, the palatine posteriorly and the septomaxilla dorsally. The anterior margin has a deep notch that forms part of the premaxillary-vomerine fenestra. The anterior portion develops a deep concavity that indicates the position of the vomeronasal organ. The posterior portion has a wide wing that extends laterally and bounds the fenestra exochoanalis. Four foramina, possibly corresponding to the lacrimal ducts, are visible in the vomer. On the posterodorsal surface, there is a defined area for the vomerine process of the palatine.

Palatine (Figs. 4N–O)

The palatine is scroll-like bone. The palatine contacts the vomer anteriorly through the vomerine process, which is approximately a quarter of the size of the entire structure. The palatine contacts the pterygoid through a slightly movable joint (probably a syndesmosis) that in other geckos has been reported to be held by fibrous tissue (Mezzasalma et al., 2013). The vomerine facet of the palatine curves inwards and covers a portion of the choanal duct. The anterolateral edge is relatively straight from the posterior end of the vomerine process down to the pterygoid process of the palatine. The lateral edge is uneven and has a marked palatine notch that might be equivalent to the palatine foramen in other species (e.g., *Sphaerodactylus roosevelti* Grant, 1931, Daza et al., 2008). In ventral view, the palatine crest is visible and runs diagonally across the palatine from the prefrontal facet down to the pterygoid process and is approximately 1 mm long. Along this crest there is a prominent deep choanal duct, which might have been covered by exochoanal cartilage, resulting in the posterior displacement of the opening of the choana in the palate.

Pterygoid (Figs. 4P–R)

The pterygoid is a large, "y"-shaped bone. It contacts the ectopterygoid anterolaterally, the palatine anteromedially, the epipterygoid dorsally, the quadrate posterolaterally, and the parabasisphenoid medially. The ectopterygoid process is long, acute, and clasped by the ectopterygoid. The anterior edge is sigmoid and the palatine process is very short and rounded. The medial margin is nearly straight, and the lateral margin runs parallel for the most part of the quadrate process. At the origin of the quadrate process, the fossa columellae receive the pterygoid process of the epipterygoid. There is a wide ovoid medial wall for the basipterygoid process, and it is possible that this joint is synovial (see Payne et al., 2011).

Epipterygoid (Fig. 4S)

This bone is columnar and extends between the pterygoid fossa columellae and the crista alaris of the prootic. The prootic process is slightly wider, where there is a distinct facet for the crista alaris. The pterygoid process is rounded and inserts into the fossa columellae. The bone shaft is compressed, and there is a small bulge on the posterior edge. There is a groove that runs through the center of the bone, but ends slightly above the ventral portion of the bone.

Ectopterygoid (Fig. 4T–U)

The ectopterygoid is flattened and crescent-shaped. It contacts the pterygoid posteriorly and has an anterolaterally ligamentous (syndesmosis) contact with the maxilla and a brief contact with the palatine anteromedially. The posterior contact with the pterygoid is firm; the ectopterygoid has a longitudinal groove posteriorly, into which the ectopterygoid process of the pterygoid fits.

Quadrate (Figs. 4V–Y)

The quadrate is a light, shell-like bone that contacts the braincase dorsomedially, the pterygoid ventromedially,

and forms part of the craniomandibular joint. The bone has an expanded dorsal portion and constriction towards the mandibular condyles. The suspension is highly modified relative to other geckos, in which the paroccipital process plays an important role. In *Pseudogonatodes barbouri,* the quadrate is streptostylic and suspended from a highly modified paroccipital process, which is flattened and shifted anteriorly, creating a small depressed area for the head of the quadrate below the bulge of the anterior ampullary recess. The suspension of the quadrate is almost ventral to the braincase, yielding a very narrow profile for the skull. The anterior surface is smooth and convex, and the posterior portion is hollow, creating a wide space for the middle ear. The medial condyle is nearly twice as big as the lateral condyle. The quadrate foramen is absent.

Sclerotic ring. (Figs. 4Z–Æ)

There are 13 ossicles of different sizes and shapes in the sclerotic ring. We followed the system of de Queiroz (1982) to number them and to indicate their position. Ossicles 1–3, 6–8, and 11 are smaller than the others and not as heavily ossified. The pattern of the ring is positive 1, 7, 10, 12 and negative 5, 11, 13, with all other ossicles gradually overlapping each other.

Otostapes (Figs. 4Þ, 4ȝ, 4Ð)

This is a very short, stout bone that fits in the fenestra ovalis, although not filling it entirely.. Its shaft is pierced, as in all sphaerodactylids, by a stapedial foramen, and its footplate is greatly reduced.

Braincase (Figs. 5A–F)

The braincase is a compact structure, as in other small sphaerodactylid geckos (Daza et al., 2008, 2012). The braincase is formed by the fusion of parabasisphenoid, basioccipital, supraoccipital, prootic and otooccipital. The dorsal border of the braincase lies almost at the same level of the parietals and postorbiotofrontals. It articulates posterolaterally with the quadrates, anteromedially with the epipterygoids, and posteriorly with the atlantoaxial complex.

The ventral portion of the braincase is formed by the basioccipital and the parabasisphenoid. These two bones form a wide concave surface. The basioccipital and the otooccipital form part of the double occipital condyle (Gardiner, 1982; Daza et al., 2008). The crista prootica is oriented anterodorsally and is very wide, extending from the basipterygoid process to the ventral margin of the foramen prootico. The anterior crista prootica extends anteriorly to the level of the lateral margin of the basipterygoid process; these two processes are long and extend anterolaterally from the posterior openings of the vidian canal. These two openings are relatively large compared to the size of other foramina in the braincase, possibly due to the combination of nerves and blood vessels that run through them. On the dorsal surface of the basipterygoid process there is a well-defined notch for the course of the lateral head vein. The groove is covered by a lamina formed by the crista prootica and the clinoid process. The basipterygoid process bears the anterior openings of the vidian canal in its base. Between the basipterygoid processes there are two small trabeculae, completely embedded in laminar bone. In the dorsomedial surface of the parabasisphenoid, the crista sellaris separates the depression for the sella turcica from the major brain concavity.

The ventral portion of the braincase has two large openings that are not concealed by the sphenooccipital tubercle as in larger gekkotans. These openings correspond to the aperture of the recessus scalae tympani, which in this species has acquired a ventral position. This opening is separated from the fenestra ovalis by a thick crista interfenestralis.

In the occiput and ventral to the posterior semicircular canal there are three foramina, corresponding to the course of the glossopharyngeal and the hypoglossal nerves. The vagus nerve foramen is visible medial to the posterior semicircular canal bulge. The dorsal surface of the supraoccipital is smooth with no indication of an ascendens tecti synotici process. The otooccipital region is characterized by the well-defined semicircular canal bulges (anterior, posterior and horizontal) and by the small paroccipital process, which is located under the horizontal semicircular canal bulge and not visible in dorsal view. The paroccipital process is located ventral to the bulge of the anterior ampullary recess and nearly dorsal to the fenestra ovalis. The anteriormost portion of the braincase is formed by the prootic, which forms the short and rounded crista alaris and encloses the foramen prootico.

Several foramina pierce the medial wall of the braincase, a large acoustic recess accommodates two conspicuous foramina for the vestibulocochlear nerve (vestibular and auditory branches). Ventral to the vestibular branch, the braincase is pierced by the facial nerve, which opens ventral to the entocarotid fossa. Posterior to the facial nerve foramen, there are two foramina, the glossopharyngeal and the endolymphatic.

Inner ear endocast (Figs. 6A–E)

The endocast of the osseous labyrinth is compact, with the semicircular canals situated very close to the vestibular and cochlear portions. The vestibule is proportionally the largest unit of the inner ear. The cochlear recess or endosseous cochlear duct (EDC) is very reduced, being approximately 1/5 the volume of the vestibule, or nearly as large as the anterior ampullar recess. Since the EDC contains the hearing organ or basilar papilla,

it is possible that these geckos have a poorly developed sense of hearing, also as indicated by the reduced otostapes. The vestibule is connected to the brain by means of the endolymphatic foramen and the two foramina for the two branches of the vestibulocochlear nerve (cranial nerve VIII). The ECD has an anterior independent duct that might correspond to the helicotrema. The endocast of *Pseudogonatodes* differs from that of semi-fossorial and semi-aquatic squamates in that the semicircular canals are not slender (Yi and Norell, 2015 ; Palci et al., 2018); on the contrary, these ducts are robust and prominent.

Dentary (Figs. 7A–C)

This is a tubular bone with a portion that cups the compound bone for about one half the length of the latter. It bears 23 pleurodont teeth that are in close contact with one another at their bases. The Meckelian canal

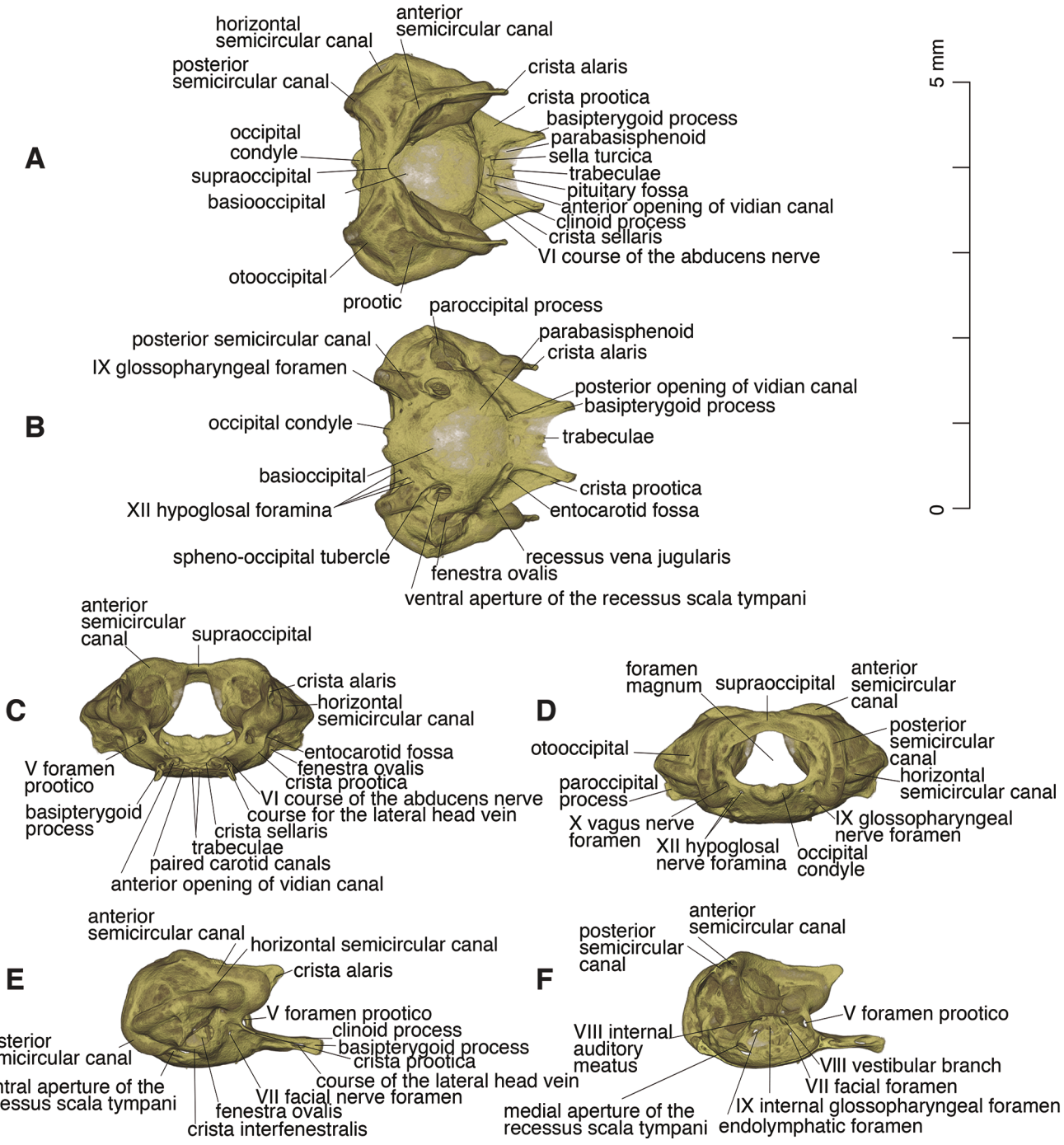

Figure 5. Basicranium of *Pseudogonatodes barbouri* (MCZ R–14385) in **(A)** dorsal, **(B)** ventral, **(C)** anterior, **(D)** posterior, **(E)** lateral, and **(F)** medial view.

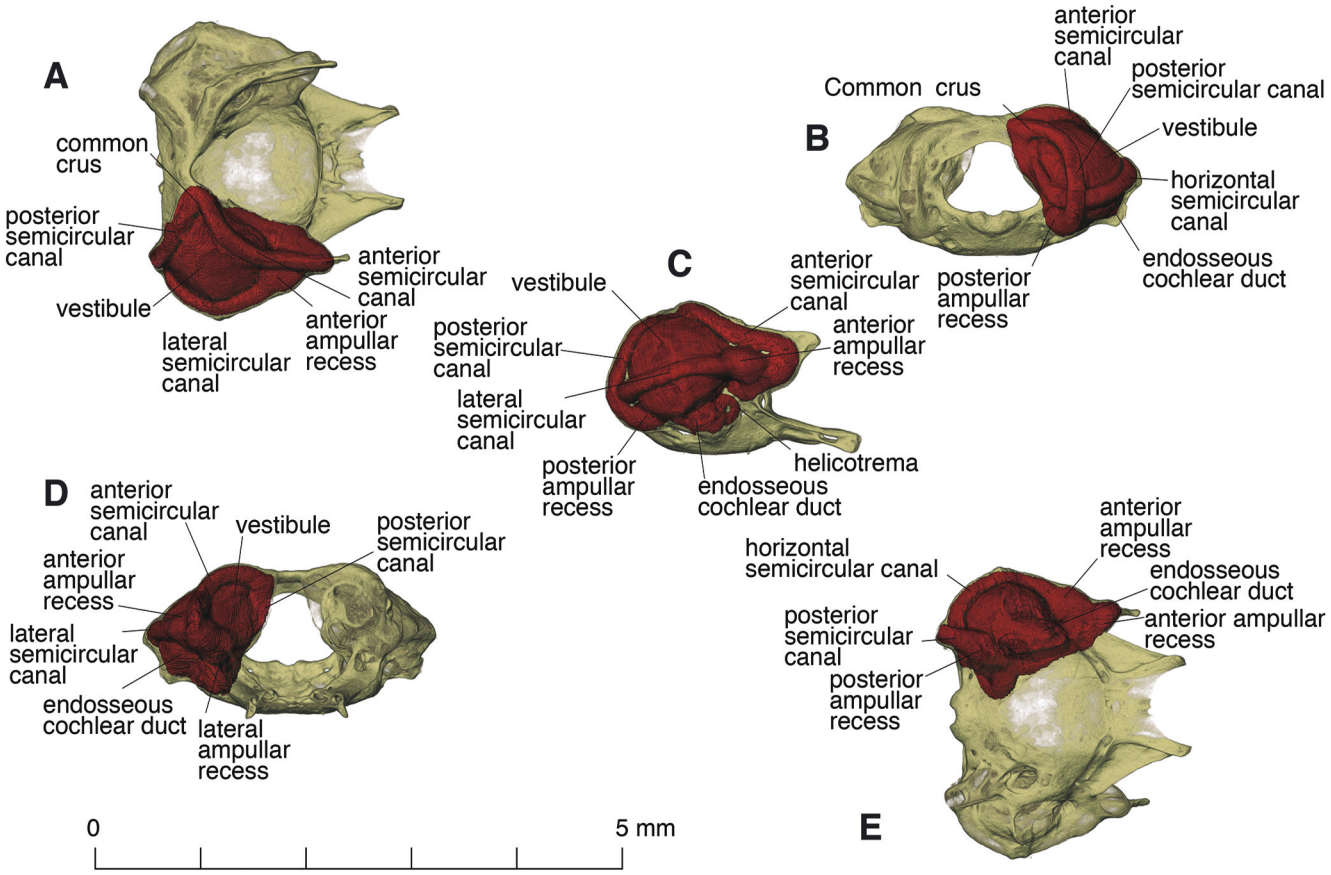

Figure 6. Inner ear endocast of *Pseudogonatodes barbouri* (MCZ R-14385) in **(A)** dorsal, **(B)** posterior, **(C)** lateral, **(D)** anterior, and **(E)** ventral view.

starts posterior to the symphyseal edge and ends just before the dorsal process, below the last mandibular tooth; from this point the medial wall is completed by the anterodorsal foot of the coronoid, which might incorporate a fused splenial. The lateral face of the dentary is flattened and has four mental foramina. The posterior region of the dentary ends into two processes, the superior (surangular) process and inferior (angular) process. There is a dorsal process behind the tooth row.

Coronoid + splenial complex (Fig. 7D–G)

The coronoid is small and loosely articulated (laminar suture) to the dentary bone and to the surangular. The coronoid is similar in shape to that described for *Sphaerodactylus roosevelti* (Daza et al., 2008). The coronoid eminence is low, not exceeding the height of the dentary teeth. Postdentary elements undergo synostosis.

Compound bone + Surangular (Figs. 7H–K)

The compound bone of *Pseudogonatodes barbouri* is very straight with an elongated retroarticular process that extends posteriorly. The retroarticular process has a rectangular shape and is rounded posteriorly, somewhat similar to a shoehorn. The surangular lies on top of the compound bone and is nearly completely fused. The surangular and the posterior surangular foramina open laterally. The external mandibular fenestra is visible dorsomedially. Just posterior to the mandibular fossa, there is a broad ovoid articular facet for the quadrate condyles. Near the base of the retroarticular process, there is a foramen for the chorda tympani, which opens medially.

Atlantoaxial complex (Figs. 8A–G)

The atlas has a broad, fused neural arch, which is anterodorsally oriented. The posterodorsal process is tubercular and pointed. The transverse process is a broad low projection located ventrolaterally. The intercentrum is short and reduced to a posteroventrally directed keel. The axis was not entirely scanned, but some diagnostic features are visible. The anterior portion of the neural spine is anterodorsally oriented and extends anteriorly to the same level of the odontoid process. The neural arch is long and the prezygapophysis is reduced to a small tubercle on the lateral side of the neural arch. The centrum is fused to the intercentrum. The latter develops some conspicuous processes, two lateral short and stout processes and two long spinelike processes. The centrum has two series of foramina (interior foramina sensu Čerňanský, 2016 or foramina subcentralis sensu Hoffstetter and Gasc, 1969).

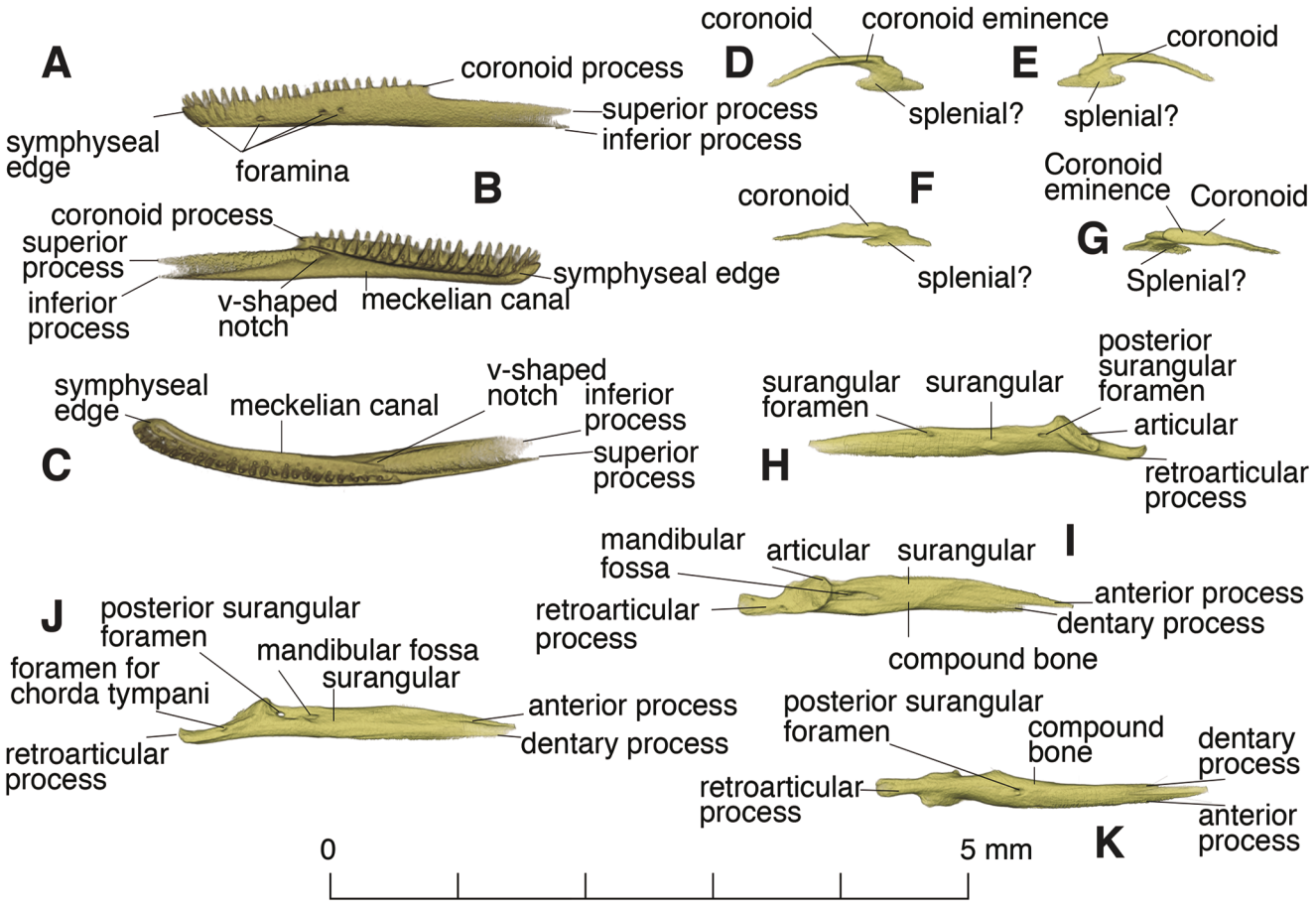

Figure 7. *Pseudogonatodes barbouri* (MCZ R-14385). Left dentary in **(A)** lateral, **(B)** medial and **(C)** dorsal view. Coronoid splenial complex in **(D)** dorsal, **(E)** ventral **(F)** medial and **(G)** lateral view. Compound bone and surangular in **(H)** lateral, **(I)** dorsal, **(J)** medial, and **(K)** ventral view.

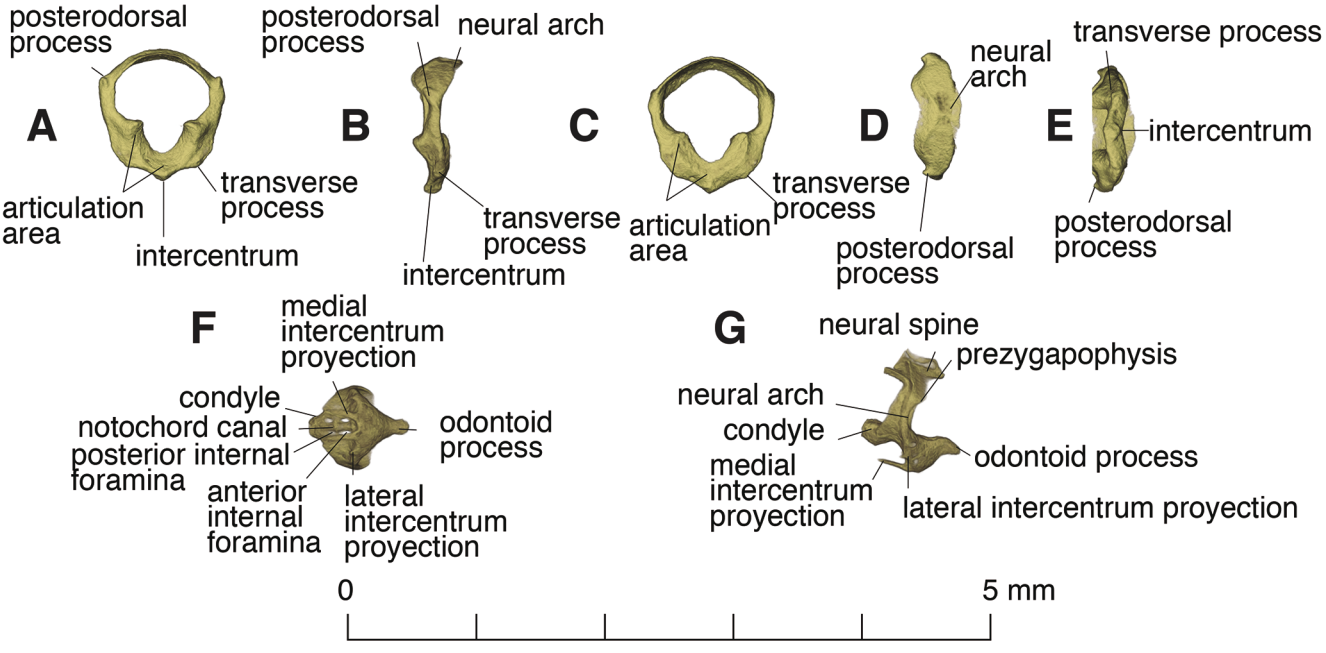

Figure 8. Atlantoaxial complex of *Pseudogonatodes barbouri* (MCZ R-14385). Atlas in **(A)** posterior, **(B)** lateral, **(C)** anterior, **(D)** dorsal, and **(E)** ventral view. Axis in **(F)** ventral and **(G)** lateral view.

The bone is so thin that the notochordal canal can be seen running across the centrum of the vertebra and ending in the odontoid process. The odontoid process is long and rounded and rests in between the occipital condyles.

DISCUSSION

The skull anatomy of *Pseudogonatodes barbouri* reflects many extreme features seen in other miniaturized gekkotans, especially closely related genera such as *Sphaerodactylus* (Daza et al., 2008) and *Chatogekko* (Gamble et al., 2011). Many of these morphological features are concentrated in the snout, especially the overlapping of the bones from the muzzle unit (Frazzetta, 1962). An illustration of the skull of *P. guianensis* (Daza et al., 2008) indicates that the genus might be characterized by having the nasal bones with expanded lateral wings and narrow posterior processes. In *Sphaerodactylus* the snout is wider and the nasals rectangular, whereas in *Chatogekko,* in which the snout becomes extremely shortened, there is huge variation in nasal shape morphology and the shape of the ascending nasal process (Wright et al., 2017). *Pseudogonatodes* shows some indication of reduction in the size of the nasals, but they do not become triangular and separated as in *Chatogekko*.

In recent molecular and morphological phylogenies of sphaerodactyls, the genus *Pseudogonatodes* has been recovered as sister to *Coleodactylus* Parker 1926 (Gamble et al., 2011) or *Chatogekko* (Daza and Bauer, 2012). Having short, compact snouts, these three South American genera are similar in morphology. They also show some similarities in the braincase anatomy, developing a globular braincase posteriorly dominated by the bulge of the lateral semicircular canal. Major changes are also present in the quadrate suspension (minor participation of the squamosal and extreme reduction of the paroccipital process), which produces an anterior shifting on the position of the quadrate. In *Pseudogonatodes,* as in *Chatogekko,* the quadrate is attached to the braincase in a very anterior position and not typical of gekkotan paroccipital abutting (Rieppel, 1984). Other structures of the braincase also are shifted anteriorly, for example, the crista prootica transformed in two large laminar wings that lie parallel to the parabasisphenoid.

Although the main foramina and fenestration of the skull is very conserved, there are some structures that have been drastically transformed as consequence of miniaturization. One of the main changes is the lateral aperture of the recessus scala tympani, which in many squamates opens laterally and ventrally to the fenestra ovalis (Evans, 2008; Olori and Bell, 2012). The jaw also shows some changes in the morphology where some of the foramina, the anterior inferior alveolar and anterior mylohyoid foramina, are no longer discrete as in other geckos (Kluge, 1962; Häupl, 1980; Daza et al., 2012). Instead these structures converge into a slit of bone between the coronoid + splenial complex and the dentary. The jaw in sphaerodactyls undergoes extreme synostosis. It has been assumed that the splenial bone is absent in sphaerodactyls, *Pristurus* Rüppell, 1835, *Ptyodactylus* Goldfuss, 1820, and *Aprasia* Gray, 1839 among gekkotans (Kluge, 1995; Kluge and Nussbaum, 1995). The morphology of the coronoid in sphaerodactyls and *Pristurus* is atypical for gekkotans, which usually have a coronoid that tapers anteroventrally into a triangular process. The anteroventral portion of the coronoid in *Pseudogonatodes,* as in other sphaerodactyls, develops a well-developed foot that takes the position of the splenial. It is possible that instead of being lost, the splenial became fused to the coronoid, or if lost, the coronoid became modified to produce the posterior walling of the Meckelian canal. An ongoing project is looking at a postnatal series of *Sphaerodactylus townsendi* Grant, 1931 using clearing and staining (J.D. Daza unpublished data), and it is possible that we can corroborate the presence of the splenial in these geckos.

The presence of a quadrate foramen is one of the more archaic features in lepidosauriomorphs (Gauthier et al., 1988); however, in *Pseudogonatodes* this foramen is absent. Absence of the quadrate foramen has been attributed to an artifact of preparation in fossils (Gauthier et al., 1988) and sometimes it is occluded in dry skulls by soft tissue (JD Daza personal observation); however, here we can confirm that it is indeed absent. It is possible that this structure was shifted dorsally towards the quadrate-otooccipital joint. In sphaerodactyls the position of the quadrate foramen fluctuates from being in near the mandibular condyles (*Sphaerodactylus roosevelti*) to a very high position near the quadrate head (*Coleodactylus brachystoma* Amaral, 1935, *Chatogekko amazonicus*) as previously illustrated elsewhere (Daza et al., 2008; Gamble et al., 2011).

The atlantoaxial complex also shows some variation on the number of ventral internal foramina compared to other species such as *Gekko gecko* Linnaeus, 1758 (Hoffstetter and Gasc, 1969). In *Pseudogonatodes* there are four foramina, as in xantusiids and cordylids (Čerňanský, 2016). The intercentrum of the axis develops the elongated and distinct finger-like processes. These processes are characteristic of sphaerodactyls, across which their size varies considerably, comparable processes are present in the agamid genus *Calotes* Cuvier, 1817, although not identical (Čerňanský, personal communication).

Today there is a large difference in the rate of generation of phenotypic versus genetic data, especially for phylogenetic analyses. Last year, Illumina announced that their new machines (HiSeq X Ten and HiSeq X Five Systems) are capable of sequencing entire genomes at incredible speeds (hours to a few days). The outcome of this project is far from producing morphological data in that time frame, but is comparatively faster than previous

projects by some of the authors of this paper (A.M. Bauer and J.D. Daza). Data collection and draft preparation started on 24 October 2017 and finished 28 November 2017. Prior to its start, squamate morphology was entirely unknown to some of the students involved. Thus, in addition to yielding rapid morphological descriptions, this approach has an important pedagogical component.

ACKNOWLEDGMENTS

For access to the paratype of *Pseudogonatodes barbouri,* we thank J. Rosado, J. Hanken and J.B. Losos at the Museum of Comparative Zoology at Harvard University. We thank J.A. Maisano and M. Colbert at the UTCT | The University of Texas High-Resolution CT Facility for scanning the specimen. We also want to thank K. Moore from the Materials & Structural Analysis division at Thermo Fisher Scientific™ for providing a trial version of the software Avizo lite 9.4. Andrej Čerňanský and an anonymous reviewer help us improving the quality of the manuscript. AMB received funding from NSF DEB 1555968 and 1556255 and the Gerald M. Lemole Endowed Chair Funds. JDD and AK received funding from NSF DEB 1657648 and the Department of Biological Sciences at Sam Houston State University.

REFERENCES

Adobe Systems Incorporated. 2017. Adobe Illustrator *CC* 22.0.1 Available from: www.adobe.com/products/illustrator.html.

Amaral A. 1935. Estudos sobre lacertilios Neotropicos. III. Um novo gênero e duas novas espécies de geckonídeos e uma nova raça de amphisbenídeo, procedentes do Brasil central. *Memórias do Instituto Butantan* 9:251–256.

Andersson L.G. 1918. New lizards from South America. Collected by Nils Holmgren and A. Roman. *Arkiv för Zoologi* 11:1–9.

Avila-Pires T.C.S. 1995. Lizards of Brazilian Amazonia (Reptilia: Squamata). *Zoologische Verhandelingen* 299:1–706.

Avila-Pires T.C.S., Hoogmoed M.S. 2000. On two new species of *Pseudogonatodes* Ruthven, 1915 (Reptilia: Squamata: Gekkonidae), with remarks on the distribution of some other sphaerodactyl lizards. *Zoologische Mededelingen* 73:209–223.

Čerňanský A. 2016. From lizard body form to serpentiform morphology: The atlas–axis complex in African cordyliformes and their relatives. *Anatomical Record* 277:512–536. DOI

Cuvier G. 1817. Le Règne Animal Distribué d'après son Organisation, pour servir de Base a l'Histoire Naturelle des Animaux et d'Introduction a l'Anatomie Comparée. Tome 2. Les Reptiles, les Poissons, les Mollusques et les Annélides. Déterville, Paris. DOI

Daza J.D., Abdala V., Thomas R., Bauer A.M. 2008. Skull anatomy of the miniaturized gecko *Sphaerodactylus roosevelti* (Squamata: Gekkota). *Journal of Morphology* 269:1340–1364. DOI

Daza J.D., Aurich J., Bauer A.M. 2012. Anatomy of an enigma: an osteological investigation of the Namibian festive gecko (*Narudasia festiva:* Gekkonidae: Gekkota). *Acta Zoologica* 93:465–486. DOI

Daza J.D., Bauer A.M. 2012. A new amber-embedded sphaerodactyl gecko from Hispaniola, with comments on the morphological synapomorphies of the Sphaerodactylidae. *Breviora* 529:1–28. DOI

de Queiroz K. 1982. The scleral ossicles of sceloporine iguanids: a reexamination with comments on their phylogenetic significance. *Herpetologica* 38:302–311.

Duke University. 2017. MorphoSource. Accessible at www.morphosource.org.

Evans S.E. 2008. The skull of lizards and tuatara. Pp. 1–347, in Gans C., Gaunt S., Adler K. (Eds.), Biology of the Reptilia, Volume 20, Morphology H. Society for the Study of Amphibians and Reptiles, Ithaca.

Frazzetta T.H. 1962. A functional consideration of cranial kinesis in lizards. *Journal of Morphology* 111:287–319. DOI

Gamble, T., Bauer, A.M., Greenbaum, E., Jackman, T.R. 2008. Evidence for Gondwanan vicariance in an ancient clade of gecko lizards. *Journal of Biogeography* 35:88–104. DOI

Gamble T., Daza J.D., Colli G.R., Vitt L.J., Bauer A.M. 2011. A new genus of miniaturized and pug-nosed gecko from South America (Sphaerodactylidae: Gekkota). *Zoological Journal of the Linnean Society* 163:1244–1266. DOI

Gasc J.P. 1976. Contribution à la connaissance des Squamates (Reptilia) de la Guyane française. Nouvelles localités pour les Sauriens. *Compte Rendu de la Societé de Biogéographie* 454:17–36.

Gardiner B.G. 1982. Tetrapod classification. *Zoological Journal of the Linnean Society* 74:207–232. DOI

Gauthier J., Estes R., de Queiroz K. 1988. A phylogenetic analysis of Lepidosauromorpha. Pp. 15–98, in Estes R., Pregill G. (Eds.), Phylogenetic relationships of the lizard families. Essays commemorating Charles L. Camp. Stanford University Press, Stanford.

Goldfuss G.A. Reptilia. Pp. 121–181. In Schubert G.H. Handbuch der Naturgeschichte zum Gebrauch bei Vorlesungen. Vol. 3. Handbuch der Zoologie. J.L. Schrag, Nürnberg.

Grant C. 1931. The sphaerodactyls of Porto Rico, Culebra and Mona islands. *Journal of the Department of Agriculture of Porto Rico* 15:199–213.

Gray J.E. 1839. Catalogue of the slender-tonged saurian, with descriptions of many new genera and species. *Annals and Magazine of Natural History* 2:331–337.

Günther A. 1859. On the reptiles from St. Croix, West Indies, collected by Messrs, A. and B. Newton. *Annals and Magazine of Natural History* 4:209–217.

Häupl V.M. 1980. Das Schädelskelett einiger Arten der Fam. Gekkonidae. *Annalen des Naturhistorischen Museums in Wien* 83:479–518.

Hoffstetter P., Gasc J.P. 1969. Vertebrae and ribs of modern reptiles. Pp. 201–310, in Gans C. (Ed.), Biology of the Reptilia, Volume 1, Morphology A. Academic Press, New York.

Kluge A.G. 1962. Comparative osteology of the eublepharid genus *Coleonyx* Gray. *Journal of Morphology* 110:299–332. DOI

Kluge A.G. 1995. Cladistic relationships of sphaerodactyl lizards. *American Museum Novitates* 3139:1–23.

Kluge A.G, Nussbaum R.A. 1995. A review of African-Madagascan gekkonid lizard phylogeny and biogeography (Squamata). *Miscellaneous Publications of the Museum of Zoology, University of Michigan* 183:1–20.

Linnaeus C. 1758. Systema naturae per regna tria naturae, secundum classes, ordines, genera, species, cum characteribus, differentiis, synonymis, locis. Tomus I. Editio decima, reformata. L. Salvii. Holmiae.

Mezzasalma M., Maio N., Guarino F.M. 2013. To move or not to move: cranial joints in european gekkotans and lacertids, an osteological and histological perspective. *Anatomical Record* 297:463–472. DOI

Noble G.K. 1921a. Some new lizards from northwestern Peru. *Annals of the New York Academy of Science* 29:133–139. DOI

Noble G.K. 1921b. The bony structure and phyletic relations of *Sphaerodactylus* and allied lacertilian genera, with the description of a new genus. *American Museum Novitates* 4:1–16.

Olori J.C., Bell C.J. 2012. Comparative skull morphology of uropeltid snakes (Alethinophidia: Uropeltidae) with special reference to disarticulated elements and variation. *PloS One* 7. DOI

Palci A., Hutchinson M.N., Caldwell M.W., Lee M.S.Y. 2018. The morphology of the inner ear of squamate reptiles and its bearing on the origin of snakes. *Royal Society Open Science* 4: 170685. DOI

Parker H.W. 1926. The Neotropical lizards of the genera *Lepidoblepharis, Pseudogonatodes, Lathrogecko,* and *Sphaerodactylus,* with the description of a new genus. *Annals and Magazine of Natural History Series 9* 17:291–301.

Parker H.W. 1935. The frogs, lizards, and snakes of British Guiana. *Proceedings of the Zoological Society of London* 1935:505–530.

Payne S.L., Holliday C.M., Vickaryous M.K. 2011. An osteological and histological investigation of cranial joints in geckos. *Anatomical Record* 294:399–405. DOI

Rieppel O. 1984. The structure of the skull and jaw adductor musculature of the Gekkota, with comments on the phylogenetic relationships of the Xantusiidae (Reptilia: Lacertilia). *Zoological Journal of the Linnean Society* 82:291–318. DOI

Rüppell E. 1835. Neue Wirbelthiere zu der Fauna von Abyssinien gehörig, entdeckt und beschrieben. Amphibien. Siegmund Schmerber, Frankfurt am Main.

Ruthven A.G. 1915. Description of a new genus and species of lizard of the family Gekkonidae. *Occasional Papers of the Museum of Zoology, University of Michigan* 19:1–3.

Ruthven A.G. 1916. A new genus and species of lizard from Colombia, with remarks on the genus *Pseudogonatodes*. *Occasional Papers of the Museum of Zoology, University of Michigan* 1916:1–3.

Thermo Fisher Scientific™. 2017. Avizo Lite 9.4. Available from: www.fei.com/software/amira-avizo.

Uetz P., Freed P., Hošek J. (Eds.). 2017. The reptile database. Accessible at www.reptile-database.org. Accessed: 27 November 2017.

Underwood G. 1954. On the classification and evolution of geckos. *Proceedings of the Zoological Society of London* 124:469–492.

Vanzolini P.E. 1957. O gênero *Coleodactylus* (Sauria, Gekkonidae). *Papéis Avulsos de Zoologia* 13:1–17.

Wagler J.G. 1830. Natürliches System der Amphibien: mit vorangehender Classification der Säugethiere und Vögel: ein Beitrag zur vergleichenden Zoologie. J.G. Cotta'scchen Buchhandlung, München, Stuttgart und Tübingen. DOI

Wright J.L., Daza J.D., Rodrigues M.T., Gamble T., Bauer A.M. 2017. Skull variation in the pug-nosed gecko *Chatogekko amazonicus* (Gekkota: Sphaerodactylidae). Abstract at Joint Meeting of Ichthyologist and Herpetologists. Austin, Texas, USA, July 12–16, 2017. Abstract 665.

Yi H., Norell M.A. 2015. The burrowing origin of modern snakes. *Science Advances* 1:e1500743. DOI